[Article ID] 1003- 6326(2001)04- 0517- 04

Thermal debinding dynamics of novel binder system①

ZHOU Ji-cheng(周继承)[1], HUANG Bai-yun(黄伯云)[1],
ZHANG Chuan-fu(张传福)[2], LIU Ye-xiang(刘业翔)[2]
(1. State Key Laboratory for Powder Metallurgy, Central South University,
Changsha 410083, P. R. China;
2. Department of Metallurgical Science and Engineering, Central South University,
Changsha 410083, P. R. China)

[Abstract] The thermal debinding dynamics of newly developed binders for cemented carbides extrusion molding was studied. It is shown that the thermal debinding processes can be divided into two stages: low temperature region, in which the low molecular mass components (LMMCs) are removed; and high temperature region, in which the polymer components are removed. The rate of thermal debinding is controlled by diffusion mechanism. The thermal debinding activation energies were solved out by differential method and integral method. The results show that the addition of other components acted as a catalyzer can effectively decrease the activation energy of thermal debinding processes.

[Key words] plasticizing powder extrusion molding; binder; thermal debinding mechanism; non-isothermal dynamics
[CLC number] TF121; TF125.3 [Document code] A

1 INTRODUCTION

Binder plays a foundational part of increasing flow and keeping shapes in the plasticizing powder extrusion molding processes[1]. Now, new binder systems[2~9] are designed with mutli-component so as to change the rheological properties and thermal debinding behaviors of binders. When a newly developed binder with reasonable formulation is designed, and the suitable rheological properties is needed for the moulding, the effects of the debinding processes on the shapes of molded bodies, on the microstructure and performance of products, on the probability and stability of technical processes must be considered[9, 10]. In this paper, the thermal debinding mechanism of binders has been researched by thermogravimetry (TG) method and differential thermogravimetry (DTG) method. The thermal debinding activation energies have been solved out by means of differential method and integnal method. This work is useful for optimizing the thermal debinding processes.

2 EXPERIMENTAL

The multi-component binders were manufactured by means of heating melting combined with solvent solving. All kinds of components were added into the mixer according to the designed formulation. And they are blended. A typical binder formulation named B_1 is: $20PS_1 + 75PW + 5SA$. The feedstock BP_1 is made of 95.4% (mass fraction) YG8 cemented carbides powders and 4.6% binder B_1. The feedstock homogeneity was judged by means of the torque-time curves.

The TG ad DTG measurements were performed for three kinds of samples, named pure polymer PS_1, binder B_1 and feedstock BP_1, respectively. The heating rate was selected and controlled to be 10 ℃/min for all samples. The experimental data were plotted into mass-temperature curves and its differential curves. In the experimental procedures, the high-purity N_2 is used, and its flux is 60 mL/min. The N_2 gas can carry away the gaseous binder which is decomposed from the sample surface.

3 RESULTS AND DISCUSSION

Fig. 1 is a group of curves of TG and DTG. Fig. 1(a) shows the removal behaviors of pure polymer PS_1, which reveals the largest debinding rate is 21.6%/min at the temperature of 477 ℃. Fig. 1(b) shows the removal behaviors of binder B_1, which reveals the two-stage debinding characteristics. During low temperature range, the LMMCs are debinded; during high temperature range, the polymer component PS_1 is removed by depolymerizing mechanism. The fastest debinding rate is 6.65%/min for LMMCs near the temperature of 280 ℃, while the fastest rate is 3.42%/min for polymer component PS_1 near the temperature of 460 ℃. Fig. 1(c) shows the TG and DTG curves of feedstock BP_1, which indicates the fastest removal rate is near 255 ℃ for the LMWCs in feedstock BP_1. This temperature is 25 ℃ lower than

① [Foundation item] Project (59634120) supported by the National Natural Science Foundation of China
[Received date] 2000- 07- 07; [Accepted date] 2000- 12- 22

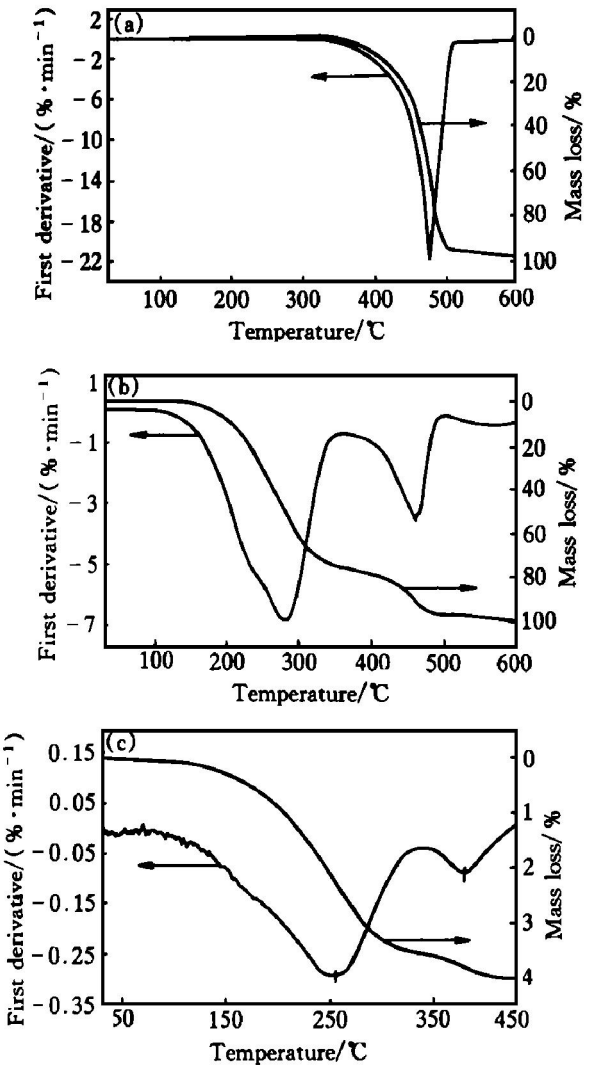

Fig. 1 TG and DTG curves of samples
(a) —PS_1; (b) —B_1; (c) —BP_1

that of pure binder B_1. For polymer PS_1 in feedstock BP_1, the fastest removal rate is near 382 ℃, this temperature is also 80 ℃ lower than that of pure binder B_1. These differences originate from the much more removal channels in feedstocks than in pure binders. The cemented carbide powders act as the dispersant, isolater and catalyzer.

4 DYNAMICS ANALYSES OF TG AND DTG CURVES

In general, there is a differential equation for reactional rates:

$$\frac{d\alpha}{dt} = f(\alpha)k(T) \tag{1}$$

where $f(\alpha)$ represents the reactional mechanism, which is the function of reactional fraction α. Table 1 lists some functions of $f(\alpha)$. $k(T)$ is the constant of reactional rate, which can be expressed by Arrhenius equation:

$$k(T) = A\exp(-E/RT) \tag{2}$$

where A is the frequency factor, E is the reactional activation energy, R is the general gas constant, and T is the absolute temperature.

From Eqns. (1) and (2), there are

$$\ln\left|\frac{d\alpha}{dt}/f(\alpha)\right| = \ln A - \frac{E}{RT} \tag{3}$$

For a given DTG curve and its data, the constant E, A for different mechanism function $f(\alpha)$ can be solved out by simulating with Eqn. (3). At the same time, the linear correlation coefficient R_L can be solved out. So the real reactional mechanism (represented by $f(\alpha)$) can be revealed. This method is called differential method for single temperature rate.

At the same time, there is an integral equation:

$$\int_0^\alpha \frac{d\alpha}{f(\alpha)} = \int_0^t A\exp(-E/RT)\,dt \tag{4}$$

The right of Eqn. (4) is a gamma function. The expression of the gamma function can't be found, which is generally solved by series method.

Here, the high accuracy expression of the gamma function made by Madhusudann[10] is used,

$$\ln\left|\frac{G(\alpha)}{T^{1.921503}}\right| = \ln\left|\frac{AE}{\beta R}\right| + 3.772050\,1 - 1.921503\ln E - \frac{E}{RT} \tag{5}$$

In Eqn. (5), $\beta = dT/dt$, represents the heating rate and $G(\alpha) = \int_0^\alpha \frac{d\alpha}{f(\alpha)}$.

For a given TG curve and its data, the activation energy E, frequency factor A can be found out from Eqn. (5). The linear correlation coefficient R_L can also be found out. This method is called integral method.

Theoretical analyses show that the reaction activation energy E_d obtained by differential method should be equal to the activation energy E_i obtained by integral method. In this paper, we think that when $|E_i - E_d|$ is minimum, the mechanism function represents the real reaction mechanism which controls the reaction process velocity. From the mathematical analyses, the linear correlation coefficient R_L can be used to criticize the simulating correctness. The value of R_L is more near ± 1, the simulation results is more correct.

By analyzing the functions of Table 1 and the DTG and TG curves in Fig. 1, the presumable reaction mechanisms are contracting volume (R_3), diffusion (D_2, D_3), first order (F_1) or second order (F_2). So, the simulations are made only for the five functions R_3, D_2, D_3, F_1, and F_2, respectively. Table 2 and Table 3 give a part of the analysis results.

By analyzing Table 2, some rules can be deduced. It is shown that the addition of powders decreases the reaction activation energy of feedstock BP_1, which acts as the catalyzer. This may be due to that the addition of powders disperses the binder

Table 1 Several kinds of mechanism function

Mechanism	$G(\alpha)$	$f(\alpha)$
Acceleratory $\alpha-t$ curve		
P_1 powder law	$\alpha^{1/4}$	$4\alpha^{3/4}$
	$\alpha^{1/3}$	$3\alpha^{2/3}$
	$\alpha^{1/2}$	$2\alpha^{1/2}$
	α	1
	$\alpha^{3/2}$	$(2/3)\alpha^{1/2}$
E_1 exponential law	$\ln\alpha$	α
S-shaped $\alpha-t$ curve		
$A_{1.5}$ Avrami-Erofeev	$[-\ln(1-\alpha)]^{2/3}$	$1.5(1-\alpha)[-\ln(1-\alpha)]^{1/3}$
A_2 Avrami-Erofeev	$[-\ln(1-\alpha)]^{1/2}$	$2(1-\alpha)[-\ln(1-\alpha)]^{1/2}$
A_3 Avrami-Erofeev	$[-\ln(1-\alpha)]^{1/3}$	$3(1-\alpha)[-\ln(1-\alpha)]^{2/3}$
A_4 Avrami-Erofeev	$[-\ln(1-\alpha)]^{1/4}$	$4(1-\alpha)[-\ln(1-\alpha)]^{3/4}$
B_1 Prout-Tompkins	$\ln[\alpha/(1-\alpha)]$	$\alpha(1-\alpha)$
	$[-\ln(1-\alpha)]^2$	$0.5(1-\alpha)[-\ln(1-\alpha)]^{-1}$
	$[-\ln(1-\alpha)]^3$	$(1/3)(1-\alpha)[-\ln(1-\alpha)]^{-2}$
	$[-\ln(1-\alpha)]^4$	$(1/4)(1-\alpha)[-\ln(1-\alpha)]^{-3}$
Deceleratory $\alpha-t$ curve		
R_2 contracting surface	$1-(1-\alpha)^{1/2}$	$2(1-\alpha)^{1/2}$
R_3 contracting volume	$1-(1-\alpha)^{1/3}$	$2(1-\alpha)^{2/3}$
D_1-1D diffusion	α^2	$1/2\alpha$
D_2-2D diffusion	$(1-\alpha)\ln(1-\alpha)+\alpha$	$-[\ln(1-\alpha)]^{-1}$
D_3-3D diffusion	$[1-(1-\alpha)^{1/3}]^2$	$1.5[1-(1-\alpha)^{1/3}]^{-1}(1-\alpha)^{2/3}$
D_4 Ginstling-Brouns	$(1-2\alpha/3)-(1-\alpha)^{2/3}$	$1.5[\ln(1-\alpha)^{-1/3}-1]^{-1}$
F_1 first order	$-\ln(1-\alpha)$	$1-\alpha$
F_2 second order	$[1/(1-\alpha)]-1$	$(1-\alpha)^2$
F_3 third order	$[1/(1-\alpha)]^2-1$	$0.5(1-\alpha)^3$

Table 2 Dynamics analysis results in low temperature region (0~ 300 ℃)

Methods	Mechanism	B_1		BP_1	
		E/(kJ·mol^{-1})	R_L	E/(kJ·mol^{-1})	R_L
Differential	R_3	38.991	−0.999 228 064	36.915	−0.999 698 185
	D_2	73.171	−0.992 556 756	47.363	−0.963 815 317
	D_3	91.531	−0.999 582 448	79.063	−0.999 953 431
	F_1	51.028	−0.995 424 006	57.428	−0.989 256 859
Integral	R_3	44.239	−0.998 138 450	33.849	−0.999 973 090
	D_2	86.077	−0.996 203 456	57.789	−0.995 928 119
	D_3	96.779	−0.999 108 343	75.997	−0.999 977 694
	F_1	49.955	−0.998 722 194	43.177	−0.996 733 438

Table 3 Dynamics analysis results in high temperature region (300~ 550 ℃)

Methods	Mechanism	PS_1		B_1	
		E/(kJ·mol^{-1})	R_L	E/(kJ·mol^{-1})	R_L
Differential	R_3	158.957	−0.979 626 960	97.393	−0.982 196 389
	D_2	276.342	−0.993 181 427	172.004	−0.984 059 350
	D_3	300.780	−0.989 685 069	233.151	−0.999 382 629
	F_1	175.100	−0.974 869 603	124.465	−0.995 637 815
	F_2	223.530	−0.963 078 834	−	−
Integral	R_3	130.497	−0.996 598 578	104.556	−0.999 768 071
	D_2	257.124	−0.998 256 576	196.274	−0.999 782 814
	D_3	272.320	−0.996 822 699	220.438	−0.999 974 477
	F_1	138.345	−0.994 686 750	117.431	−0.998 200 153
	F_2	164.556	−0.986 913 821	−	−

moleculae, which effectively decreases the joining degree of binds moleculae. By the above two criteria, that is E_d should be equal to E_i, and R_L should be near ± 1, it can be deduced that the thermal debinding mechanism of binder B_1 and feedstock BP_1 is three dimension diffusion during the low temperature region (0~ 300 ℃), the activation energy is 94.2 kJ/mol for binder B_1, while the activation energy is 77.5 kJ/mol for feedstock BP_1. These conclusions show again the thermal debinding rules just shown in Ref. [1].

From Table 3, it can be concluded that the thermal debinding mechanism for pure polymer PS_1 is two dimensional diffusion, the activation energy is 266.7 kJ/mol. For binder B_1 in which there are some polymer component PS_1, the thermal debinding process is more easy, the activation energy is 226.6 kJ/mol and the mechanism is three dimensional diffusion. In fact, the pure polymer PS_1 possesses the shape of column, of course, its diffusion mechanism shows the two-dimensional state. But when the polymer PS_1 is mixed with some LMMCs by heating melting and solvent solving, the polymer component PS_1 possesses the isotropic states and the diffusion mechanism show the three dimensional diffusion.

5 CONCLUSIONS

1) The TG and DTG analyses of samples show that the thermal debinding of the binder and feedstock can be divided into two stages: low temperature region (0~ 300 ℃), in which the LMWCs is removed; high temperature region (300~ 550 ℃), in which the polymer component PS_1 is removed. This characteristic is very useful for the debinding technical processes establishing and controlling.

2) In low temperature region, the thermal debinding reaction activation energies for binder B_1 and feedstock BP_1 are 94.2 kJ/mol and 77.5 kJ/mol, respectively; while in high temperature region, the energies for polymer component PS_1 and binder B_1 are 266.7 kJ/mol and 226.6 kJ/mol, respectively. The dynamics analyses for TG and DTG curves show that the addition of other components as the catalyzer can effectively decrease the thermal-debinding reaction activation energy.

3) All dynamic simulating results show that the thermal debinding mechanisms for pure polymer PS_1, binder B_1 and feedstock BP_1 are diffusion. Pure polymer PS_1 possesses the shape of column, whose thermal debinding mechanism is two-dimension diffusion. But for polymer component PS_1 in binder B_1 and feedstock BP_1, the thermal debinding mechanism is three-dimensional diffusion, because the polymer component PS_1 in B_1 and BP_1 possesses the isotropic states.

4) It should be emphasized that the heating rate must be controlled strictly in the low temperature region, in order to avoid producing defects, such as tympanic, and crazing. This is because that in the low temperature region, the debinding process is just beginning, the LMWCs is melting, diffusing, volatilizing, the holes in the molded bodies are little and small and the activation energy is smaller than that in the high temperature region.

[REFERENCES]

[1] ZHOU J C, HUANG B Y, WU E X, et al. Thermal debinding of a new binder [J]. Trans Nonferrous Met Soc China, 1997, 7(4): 107.

[2] Friedrichs K A. New technology for the production of carbide rods with helical twisted coolant holds [A]. Bildstein H, Eck R. Proc of 13th Plansee Seminar [C]. RWF, Werbegesellschaft m. b. h., Wattens, Austria, 1993, 2: 468.

[3] Friedrichs I A. New plastification agent for the extrusion molding of sintered carbide rods with cooling channel borings [A]. Bildstein H, Ortner H M. Proc of 14th Plansee Seminar [C]. RWF, Werbegesellschaft m. b. h., Wattens, Austria, 1995, 1: 321.

[4] Shaw H M, Edirisihghe M J. A model for the diffusion of organic additives during thermolysis of a cermaic body [J]. Philosophical Magazine A, 1995, 72(1): 267.

[5] Pinwill I E. Development of temperature-heating rate diagrams for the pyrolytic removal of binder [J]. J Mater Sci, 1992, 27: 4381.

[6] Angermann H H, Biest O V. Low temperature debinding kinetics of two-component model systems [J]. Int J Powder Metall, 1993, 29(3): 239.

[7] German R M. Theory of thermal debinding [J]. Int J Powder Metall, 1987, 23(4): 237.

[8] ZHOU J C, HUANG B Y, WU E X, et al. Rheological and thermal degreasing characteristics of novel formative agent [J]. The Chinese Journal of Nonferrous Metals, (in Chinese), 1998, 8(4): 647.

[9] Moller J C, Lee D. Constitutive behavior of a powder/binder system: molding and thermal debinding [J]. Int J Powder Metall, 1994, 30(1): 103.

[10] Madhusudanan P M, Krishnan K, Ninan K N. New approximation for the $p(x)$ function in the evaluation of non-isothermal kinetic data [J]. Thermochimica Acta, 1986, 97: 189.

(Edited by YUAN Sai-qian)